Liquid Crystals
Publication details, including instructions for authors and subscription information:
http://www.informaworld.com/smpp/title~content=t713926090

Comparison of short range interactions in nematic liquid crystals A ^{2}H-NMR study of 5CB-d_{19} as a solute

T. Chandrakumar[a]; Dan S. Zimmerman[a]; G. S. Bates[a]; E. Elliott Burnell[a]
[a] Department of Chemistry, University of British Columbia, Vancouver, B.C., Canada

To cite this Article Chandrakumar, T. , Zimmerman, Dan S. , Bates, G. S. and Burnell, E. Elliott(1994) 'Comparison of short range interactions in nematic liquid crystals A ^{2}H-NMR study of 5CB-d_{19} as a solute', Liquid Crystals, 17: 4, 457 — 485
To link to this Article: DOI: 10.1080/02678299408036733
URL: http://dx.doi.org/10.1080/02678299408036733

LIQUID CRYSTALS, 1994, VOL. 17, NO. 4, 457–485

Comparison of short range interactions in nematic liquid crystals
A ^{2}H-NMR study of 5CB-d_{19} as a solute

by T. CHANDRAKUMAR, DAN S. ZIMMERMAN, G. S. BATES
and E. ELLIOTT BURNELL*

Department of Chemistry, University of British Columbia,
2036 Main Mall, Vancouver, B.C., Canada V6T 1Z1

(*Received 22 June 1993; accepted 18 October 1993*)

Previous studies using dideuterium as a solute have demonstrated the importance for orientation of the interaction between the solute molecular quadrupole moment and the average electric field gradient present in liquid crystals. With the aim of learning about additional orientational mechanisms, we have studied the temperature dependence of the ^{2}H-NMR spectra of the liquid crystal 5CB-d_{19} as the solute in three liquid crystal mixtures: 55 wt % 1132/EBBA, 56·5 wt % 1132/EBBA and 70 wt % 5CB/EBBA. In these mixtures, the contribution from the environment to the average electric field gradient at the ^{2}H nucleus of dideuterium is zero. The spectra of 5CB-d_{19} in the mixtures 55 wt % 1132/EBBA and 56·5 wt % 1132/EBBA are equivalent, but are different from those in 70 wt % 5CB/EBBA. The spectra of 5CB in 55 wt % 1132/EBBA and 70 wt % 5CB/EBBA are analysed using two different models for the short range potential, and parameters of the models are used to compare the potentials in the different mixtures. For a given spectral splitting of the chain C_1 deuteron, the reduced short range potential is the same in all three mixtures studied. The spectral differences observed are a consequence of different nematic–isotropic phase transition temperatures combined with the effect of *trans/gauche*-isomerization in the hydrocarbon chain.

1. Introduction

A detailed understanding of anisotropic intermolecular interactions leading to orientational ordering in liquid crystal systems is not available. The situation is complicated by the size and flexibility of the liquid crystal molecules. In many cases, the intermolecular interactions are described by a mean field theory [1–3] in which the interaction potential is expressed in terms of model parameters.

The anisotropic interactions lead to an orientational ordering of the liquid crystal molecules. This orientational ordering can be described in terms of order parameters. Second rank order parameters can be measured by various techniques, including NMR (nuclear magnetic resonance) spectroscopy. NMR measurements can also be used to obtain information about order parameters of solutes in liquid crystal solvents [4, 5].

The use of small solutes in liquid crystal solvents has provided a useful route for investigating the intermolecular interactions in these systems. In the past, our group has proposed two important mechanisms for the intermolecular interactions acting between the solute and the liquid crystal molecules. First, the electric quadrupole moment of the solute interacts anisotropically with the average electric field gradient that the solute experiences in the liquid crystal environment. The second mechanism involves short range interactions that depend on the size and shape of the solute [6, 7].

* Author for correspondence.

0267–8292/94 $10·00

To investigate the short range interactions, it is useful to use systems in which the average electric field gradient is negligibly small. Our group has shown that the molecule D_2 can be used to measure the average electric field gradients of liquid crystal solvents [8, 9]. Measurements have been carried out for several nematic liquid crystal solvents including *N*-4-ethoxybenzylidene-4′-*n*-butylaniline (EBBA) and the mixture Merck ZLI 1132. The signs of the electric field gradients in these two liquid crystal solvents are opposite, and thus a mixture of the two can yield a liquid crystal combination in which the average electric field gradient as seen by the ^2H nucleus vanishes. In particular, the measured electric field gradient is zero for a mixture of 55 wt% 1132/EBBA at 301·4 K [8]. Other studies [10] show that the solute methane also experiences an average zero electric field gradient in this mixture. Extensive studies of small and large solutes, including mesogenic molecules such as 1CB and 5CB, were undertaken to investigate the short range interactions in this mixture [11, 12]. Simple models for the short range interactions were very successful in rationalizing the results obtained [12, 13]. However, it is crucial to ask whether these models are specific for this one special mixture, or whether they provide a reasonable description of the anisotropic short range interactions in nematic liquid crystals in general. Therefore, it would be interesting to examine a series of liquid crystal mixtures in which D_2 experiences a zero electric field gradient, and to see to what extent the description of the short range interactions is the same or differs in these mixtures. We shall refer to these special mixtures, in which the measured electric field gradient is zero, as zero efg mixtures. Such mixtures experience a zero efg at a precise temperature; at other temperatures there exists a small non-zero efg. However, we shall see that this small efg does not significantly affect our results. Therefore, throughout this paper, we shall use the term zero efg mixture to include the nematic temperature range of a mixture that exhibits a zero efg at some temperature within this range.

There are several possibilities for investigating zero efg mixtures. One is to use the same combination of liquid crystals such as 1132 and EBBA, but vary the composition. For example, Barnhoorn *et al.* [14], investigated 56·5 wt% 1132/EBBA using D_2 as a solute and found that the average electric field gradient is zero at 322 K. Another possibility is to choose a different pair of liquid crystals which have average electric field gradients of opposite sign. As one of the components it would be interesting to use the liquid crystal 5CB (4-*n*-pentyl-4′-cyanobiphenyl), a relatively simple nematic liquid crystal that has received a lot of experimental and theoretical attention from the NMR community [15–22]. D_2 has been used to measure the electric field gradient in this liquid crystal at various temperatures [22]. The magnitude of the average electric field gradient in 5CB is found to be 30 per cent as large as that observed in EBBA, but of opposite sign. This suggests that the electric field gradient should be zero in a mixture of 5CB and EBBA. A study of D_2 dissolved in the liquid crystal mixture 70 wt% 5CB/EBBA shows that its measured electric field gradient is zero at 316 K [14].

In this paper, the molecule 5CB-d_{19} (see figure 1) that by itself forms a nematic liquid crystal and is a component of one of the mixtures is studied in the three zero efg mixtures 55 per cent† 1132/EBBA, 56·5 per cent 1132/EBBA and 70 per cent 5CB/EBBA. These systems allow us to ignore the electric quadrupole moment–electric field gradient interaction in the mean-field potential. We shall assume that only short range interactions contribute to the anisotropic intermolecular potential in these special mixtures. For our analysis, we shall use two of the simple models for short range

† Throughout this paper composition of all mixtures refers to wt%.

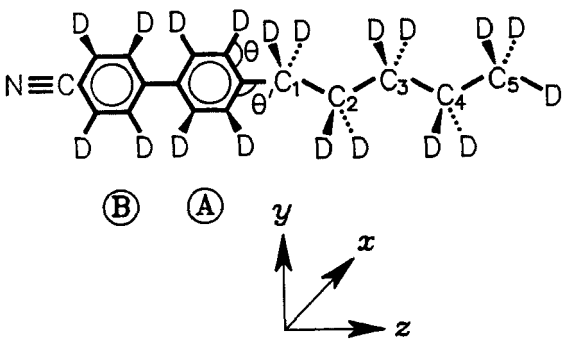

Figure 1. The coordinate system and atom numbering scheme of the 5CB-d_{19} molecule.

interactions that were developed [13, 23] to explain data on solutes in the 55 wt% 1132/EBBA mixture. The spectra of 5CB-d_{19} are not the same in the different mixtures. In this paper we shall demonstrate that the short range potential can be described in the same way in all three mixtures—the spectral differences arise from the differing effects of temperature on the different parts of the potential.

2. Review of theory

The solute 5CB-d_{19} has a rigid ring part and a flexible chain part. According to the RIS approximation [24], each C–C bond has three discrete rotational states: *trans*, *t*, and two *gauche*, $g+$ and $g-$. Thus, there are 27 conformer states for 5CB-d_{19}. The total energy, $U_{T,i}(\Omega)$, of conformer i in orientation Ω is a sum of two terms [25]

$$U_{T,i}(\Omega) = U_{\text{int},i} + U_i(\Omega). \tag{1}$$

$U_{\text{int},i}$, which is assumed to be independent of orientation [26], describes the internal energy of conformer i. $U_i(\Omega)$ is an orientation dependent part of the interaction potential. The internal energy, $U_{\text{int},i}$, is given by

$$U_{\text{int},i} = n_g E_{tg} + n_{g+g-} E_{g+g-}, \tag{2}$$

where E_{tg} is the *trans–gauche* energy difference, n_g is the number of *gauche* rotations and n_{g+g-} is the number of *gauche* + followed by *gauche* − rotations in the conformer. The energy E_{g+g-} is the additional energy required to inhibit successive *gauche* + *gauche* − bonds which include large steric interactions. E_{g+g-} is taken as 1·5 kcal mol^{-1} [12]. The probability of conformer i, p_i, is given by

$$p_i = \frac{\exp\left(\frac{-U_{\text{int},i}}{kT}\right)\int \exp\left(\frac{-U_i(\Omega)}{kT}\right) d\Omega}{\sum_i \exp\left(\frac{-U_{\text{int},i}}{kT}\right)\int \exp\left(\frac{-U_i(\Omega)}{kT}\right) d\Omega} \tag{3}$$

where the integration is over all orientations Ω. For a nematic liquid crystal with the director aligned parallel to the magnetic field direction, the quadrupolar splitting of a deuteron in conformer i, $\nu_{Q,i}$, is given by

$$\nu_{Q,i} = \sum_\alpha \sum_\beta \frac{e^2 Q}{h} q_{\alpha\beta,i} S_{\alpha\beta,i} \tag{4}$$

where eQ is the quadrupole moment of the ^{2}H nucleus, $S_{\alpha\beta,i}$ and $q_{\alpha\beta,i}$ are the $\alpha\beta$

components of the order matrix and the electric field gradient of the deuteron nucleus in a conformer coordinate frame. The components of the order matrix for conformer i, $S_{\alpha\beta,i}$, are given by

$$S_{\alpha\beta,i} = \frac{\int (3\cos\theta_\alpha \cos\theta_\beta - \delta_{\alpha\beta}) \exp\left(\frac{-U_i(\Omega)}{kT}\right) d\Omega}{2\int \exp\left(\frac{-U_i(\Omega)}{kT}\right) d\Omega}, \tag{5}$$

where $\cos\theta_\alpha$, $\cos\theta_\beta$ are the direction cosines of the α, β axes with respect to the Z, director, axis. The calculated quadrupolar splitting, $\Delta\nu_Q$, is then

$$\Delta\nu_Q = \sum_i \nu_{Q,i} p_i \tag{6}$$

The principal axes, a, b, c, of the intramolecular electric field gradient tensor of the ring deuterons have axis b along the C–D bond and axis a in the plane of the ring. The quadrupolar splitting of conformer i, $\nu_{Q,i}$, is then written in terms of the quadrupolar coupling constant, e^2Qq_{bb}/h, and the asymmetry parameter, $\eta = (q_{aa} - q_{cc})/q_{bb}$. The quadrupolar coupling constant for ring deuterons is 185 kHz, and η is 0·04 [12]. For the flexible chain part, the quadrupolar coupling constant is taken as 168 kHz and η is taken as zero [12].

In order to calculate the quantities p_i, $S_{\alpha\beta,i}$ and hence $\Delta\nu_Q$, information about both the $U_i(\Omega)$ and $U_{\text{int},i}$ is necessary. According to [6], the interaction potential, $U_i(\Omega)$, can be written as a sum of the electric field gradient–electric quadrupole moment interaction potential and a short range interaction potential, $U_{\text{sr},i}(\Omega)$. In zero electric field gradient mixtures, the interaction potential, $U_i(\Omega)$, is assumed to be equal to the short range potential, $U_{\text{sr},i}(\Omega)$. Since the nature of the short range potential is not known exactly, we shall use models for it. These will be reviewed in the Discussion section.

3. Experimental

The liquid crystal ZLI 1132, which is a eutectic mixture of alkylcyclohexylcyanobenzenes and alkylcyclohexylcyanobiphenyls, was purchased from E. Merck, Darmstadt and was not purified prior to use. The liquid crystal EBBA was synthesized in Amsterdam using the procedure given in [27]. The liquid crystal 5CB was purchased from Merck Ltd, U.K. The liquid crystals 1132, EBBA and 5CB were used to prepare the liquid crystal mixtures 70 wt% 5CB/EBBA, 55 wt% 1132/EBBA and 56·5 wt% 1132/EBBA. The solute 5CB-d_{19} was synthesized at UBC [12]. 1–2 wt% of 5CB-d_{19} as solute was dissolved in each liquid crystal mixture, the mixture heated to the isotropic phase, and mixed using a vortex stirrer. The sample was subjected to freeze–pump–thaw cycles until no gas evolved from the liquid crystal mixture. The samples were transferred to NMR tubes, and the tubes were flame sealed under vacuum. Quadrupolar echo excitation was used to run the NMR experiment on a Bruker CXP-200 NMR spectrometer operating at 30·76 MHz for ^{2}H nuclei. Spectra were obtained by Fourier transforming from the top of the echo [28]. The experiment was repeated as a function of temperature from the solid to the isotropic phase region for all three liquid crystal mixtures.

Separate microscope slides were prepared from the pure solvents 55 per cent 1132/EBBA and 70 per cent 5CB/EBBA, and were studied using a Leitz Laborlux 12POL polarizing microscope equipped with a Mettler FP2 heating stage by Dr Mary E. Neubert at Kent State University to determine the phase transitions of

these zero efg mixtures. It was found that T_{NI}, the nematic–isotropic transition temperature, of 55 per cent 1132/EBBA is in the range 341·8 K to 342·4 K, and that T_{NI} of 70 per cent 5CB/EBBA is in the range 320·6 K to 321·4 K. It was also found that all three liquid crystal mixtures used in this study are in the nematic phase over the temperature range used for the NMR experiments.

4. Results

The NMR spectrum of 5CB-d_{19} in zero efg solvents has seven pairs of quadrupolar lines, each pair corresponding to a different C–D bond site. Figure 2 shows the spectra of 5CB-d_{19} in 55 per cent 1132/EBBA at 307·1 K and in 70 per cent 5CB/EBBA at 306·8 K. The quadrupolar lines are broadened due to the dipole–dipole coupling between deuterons. Quadrupolar splittings were measured in a manner consistent with line shape simulations. Measurements were carried out at temperatures ranging from 250 K to the isotropic temperature on the mixtures 55 per cent 1132/EBBA, 70 per cent 5CB/EBBA and 56·5 per cent 1132/EBBA. Measured line positions are tabulated in tables 1 to 3. Spectral line assignments were based on previous work [29] and are in agreement with predictions from our calculations below.

As the temperature approaches T_{NI}, the spectra begin to appear as a superposition of nematic and isotropic peaks. The lowest temperature at which the isotropic peak appears is taken to be T_{NI}. The T_{NI} of 55 per cent 1132/EBBA and 56·5 per cent 1132/EBBA are 337 K and 339 K, respectively, and the T_{NI} of 70 per cent 5CB/EBBA is 316 K. These numbers differ slightly from those above because the samples used for NMR contain deuteriated materials.

The measured quadrupolar splittings at position 1, $\Delta\nu_1$, are plotted against temperature in figure 3. The curves corresponding to 55 per cent 1132/EBBA and 56·5 per cent 1132/EBBA are similar. However, the curve corresponding to the mixture 70 per cent 5CB/EBBA appears to have a break at 307 K (see figure 3). Below this temperature the quadrupolar splitting changes linearly with temperature. However, the microscope study indicates that there is no phase transition taking place near 307 K in this mixture. Thus, the liquid crystal mixtures are nematic for all points given in figure 3.

5. Discussion

5.1. *General*

The purpose of this paper is to examine several zero efg mixtures and to investigate the short range potentials in these mixtures. In addition we shall investigate to what extent the description of the anisotropic short range potential is similar or is different in the various mixtures. One way of emphasizing small differences among the zero efg mixtures is to plot ratios of the quadrupolar splittings, such as $\Delta\nu_5/\Delta\nu_1$, against $\Delta\nu_1$. These plots shall be referred to as ratio plots. Ratio plots for 5CB-d_{19} were previously used to illustrate differences among the liquid crystals 1132, EBBA, 5CB and 55 per cent 1132/EBBA [12]. In that study, the differences were ascribed to the presence of a non-zero electric field gradient in the various liquid crystals.

A plot of $\Delta\nu_5/\Delta\nu_1$ against $\Delta\nu_1$ is shown in figure 4. Intuitively, one might expect that ratio plots for all zero efg mixtures would be similar. However, the differences between 55 per cent 1132/EBBA and 70 per cent 5CB/EBBA are large and comparable to those between the liquid crystals 1132 and EBBA in [12]. On the other hand, the ratio plots of 5CB-d_{19} in 55 per cent 1132/EBBA and in 56·5 per cent 1132/EBBA are

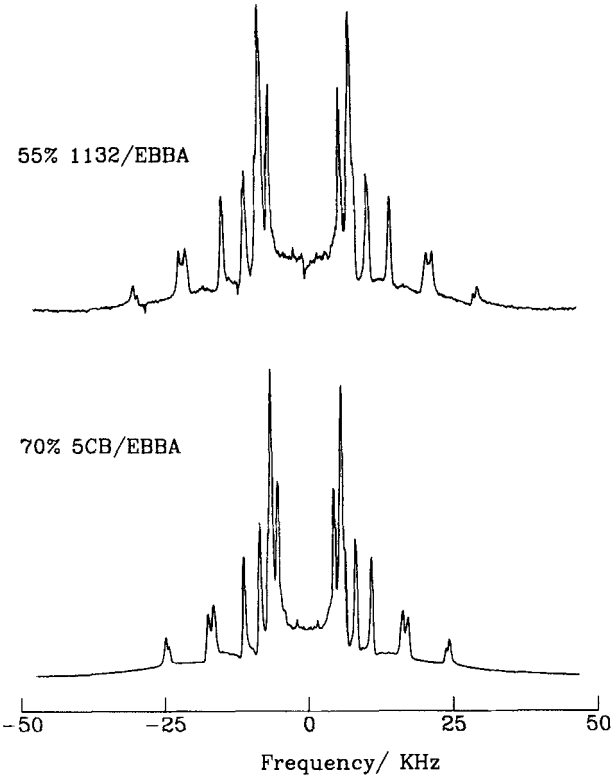

Figure 2. Experimental ^{2}H-NMR spectra of 5CB-d_{19} dissolved in the zero efg mixtures 55 per cent 1132/EBBA, at 307·1 K, and 70 per cent 5CB/EBBA at 306·8 K.

Table 1. Quadrupolar splittings (in kHz) of 5CB-d_{19} in 55 per cent 1132/EBBA.

Temperature/K	$\Delta\nu_1$	$\Delta\nu_2$	$\Delta\nu_3$	$\Delta\nu_4$	$\Delta\nu_5$	Ring *A*	Ring *B*
251·4	77·782	63·768	65·233	49·559	35·790	21·728	17·577
256·1	77·050	62·255	63·719	47·899	34·569	21·435	17·430
261·1	75·878	60·887	62·597	46·142	33·446	21·240	17·236
265·3	75·048	59·569	61·327	44·823	32·568	20·946	17·040
270·7	74·267	58·251	59·960	43·066	31·396	20·946	16·893
275·8	73·974	57·177	58·739	41·747	30·663	20·702	16·699
281·5	72·314	55·028	56·688	39·745	29·199	20·263	16·161
285·3	70·898	53·319	55·077	38·329	28·173	19·725	15·721
292·1	68·309	50·438	52·489	35·936	26·366	18·896	14·941
296·4	66·796	48·730	50·634	34·520	25·292	18·310	14·501
302·1	64·697	46·337	48·339	32·616	23·827	17·577	13·818
307·1	62·743	44·189	46·239	30·858	22·606	16·698	13·232
312·7	59·911	41·308	43·456	28·612	20·995	15·770	12·352
317·0	57·079	38·768	41·014	26·757	19·579	14·843	11·572
323·1	53·368	35·448	37·646	24·218	17·724	13·524	10·497
327·0	49·316	32·079	34·276	21·776	15·917	12·255	9·325
332·6	42·333	26·806	28·661	18·017	13·182	10·156	7·567
334·6	36·622	24·315	25·927	16·307	11·962	9·130	6·786

Table 2. Quadrupolar splittings (in kHz) of 5CB-d_{19} in 70 per cent 5CB/EBBA.

Temperature/K	$\Delta\nu_1$	$\Delta\nu_2$	$\Delta\nu_3$	$\Delta\nu_4$	$\Delta\nu_5$	Ring *A*	Ring *B*
251·9	72·509	57·812	59·569	44·140	32·031	19·725	15·966
255·9	70·702	55·663	57·958	42·626	30·956	19·189	15·526
261·2	69·579	53·564	55·712	40·233	29·345	18·652	14·940
265·3	68·163	52·148	54·101	38·720	28·271	18·212	14·550
271·1	65·868	49·511	51·513	36·230	26·513	17·528	13·963
276·1	64·550	47·704	49·755	34·569	25·438	17·040	13·524
281·9	62·108	44·921	46·972	32·177	23·827	16·258	12·841
285·9	60·399	43·017	45·116	30·517	22·704	15·721	12·352
292·1	57·861	40·331	42·626	28·319	21·044	15·038	11·766
296·6	56·298	38·671	40·819	26·854	20·018	14·452	11·425
302·0	53·906	36·620	38·573	24·999	18·700	13·866	10·937
306·8	51·563	34·570	36·524	23·438	17·480	13·232	10·400
308·8	49·462	32·909	34·813	22·118	16·551	12·597	9·764
310·8	46·728	30·859	32·714	20·702	15·477	11·816	9·130
312·7	42·968	28·026	29·736	18·700	14·013	10·595	8·153
313·7	40·624	24·464	28·075	17·578	13·134	10·008	7·616
314·7	37·646	24·608	25·976	16·210	12·059	9·228	6·982
315·7	34·130	21·678	22·704	14·404	10·839	8·104	6·201

Table 3. Quadrupolar splittings (in kHz) of 5CB-d_{19} in 56·5 per cent 1132/EBBA.

Temperature/K	$\Delta\nu_1$	$\Delta\nu_2$	$\Delta\nu_3$	$\Delta\nu_4$	$\Delta\nu_5$	Ring *A*	Ring *B*
261·4	75·927	61·156	62·987	46·569	33·691	21·239	17·211
266·1	75·255	59·997	61·827	45·349	32·714	20·995	16·966
271·7	74·340	58·287	60·180	43·334	31·616	20·812	16·783
276·0	73·791	57·311	59·143	42·236	30·821	20·751	16·722
281·9	72·630	55·480	57·067	40·160	29·479	20·201	16·234
286·1	71·044	53·649	55·541	38·695	28·441	19·713	15·929
292·5	69·029	50·963	53·222	36·620	26·854	19·042	15·075
296·7	67·321	49·133	51·390	35·095	25·634	18·432	14·587
302·0	65·123	46·813	48·889	33·080	24·169	17·638	13·915
307·1	63·415	44·615	46·752	31·372	22·887	16·844	13·304
312·6	60·851	41·870	44·249	29·235	21·362	15·990	12·511
317·1	58·226	39·489	41·869	27·403	20·018	15·075	11·718
323·1	54·686	36·376	38·513	24·963	18·249	13·854	10·742
327·6	50·963	33·263	35·522	22·704	16·600	12·633	9·764
328·6	50·109	32·653	34·972	22·277	16·234	12·389	9·459
330·1	48·095	31·127	33·202	21·117	15·380	11·779	8·971
330·6	47·057	30·089	32·226	20·446	14·892	11·413	8·666
332·6	44·799	28·502	30·517	19·286	14·037	10·802	8·056
333·6	43·578	27·648	29·601	18·676	13·610	10·436	7·812
334·6	42·296	26·732	28·747	18·065	13·183	10·070	7·507
335·1	40·526	25·573	27·465	17·272	12·572	9·642	7·140
336·1	38·207	23·864	25·817	16·112	11·718	8·971	6·591
337·1	36·193	22·460	23·925	15·075	11·046	8·300	6·163
338·1	33·019	20·263	21·422	13·732	10·009	7·446	5·553

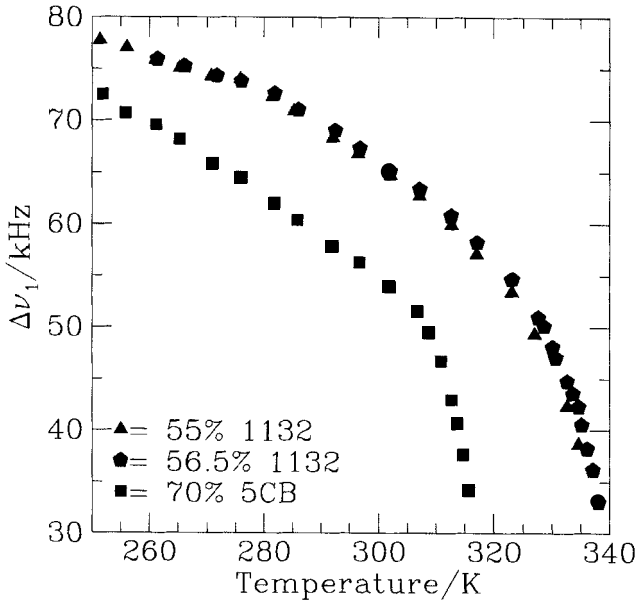

Figure 3. The quadrupolar splitting $\Delta\nu_1$ versus temperature for the mixtures 55 per cent 1132/EBBA, 70 per cent 5CB/EBBA and 56·5 per cent 1132/EBBA.

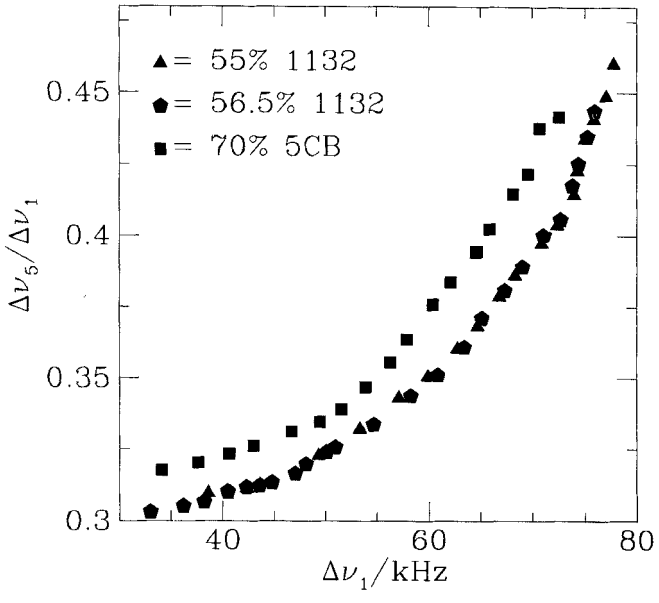

Figure 4. Quadrupolar splitting ratios $\Delta\nu_5/\Delta\nu_1$ versus $\Delta\nu_1$ of 5CB-d_{19} in the zero efg mixtures 55 per cent 1132/EBBA, 70 per cent 5CB/EBBA and 56·5 per cent 1132/EBBA.

superimposable. This latter fact allows us to evaluate the effect of a small residual electric field gradient present in the mixtures 55 per cent 1132/EBBA and 56·5 per cent 1132/EBBA at temperatures other than 301·4 K and 322 K where the electric field gradient is zero.

In such zero efg mixtures, the average electric field gradient measured using D_2 changes sign and magnitude with changing temperature. At any given temperature, the average electric field gradient in the 55 per cent 1132/EBBA mixture differs from that in the 56.5 per cent 1132/EBBA mixture. If these small efg's made a significant contribution to the anisotropic orientational potential, the ^{2}H spectra of 5CB-d_{19} should differ between the two mixtures. However, the ratio plots in figure 4 show that the quadrupolar splitting ratios $\Delta\nu_5/\Delta\nu_1$ are identical for the two mixtures over the temperature range 250–337 K. This result, together with the equivalence of the $\Delta\nu_1$ for the two 1132/EBBA mixtures in figure 3, shows that the small electric field gradients present in these mixtures have a negligible effect on the spectra. The quadrupole moment–electric field gradient mechanism can be neglected as an important orientational mechanism in these mixtures. Thus, when we refer to a zero efg mixture, we include the entire nematic range of a mixture that has a precisely zero efg at one specific temperature. Note that van der Est *et al.* [30], have reported a quantitative temperature and concentration dependence study of the efg in 1132/EBBA mixtures.

We shall also assume that the contribution of the electric field gradient–electric quadrupole moment interaction to $U_{T,i}(\Omega)$ is negligible throughout the nematic range of the zero efg mixture 70 per cent 5CB/EBBA. Thus the differences in figure 4 between 70 per cent 5CB/EBBA and the other zero efg mixtures do not arise from the electric field gradient–molecular quadrupole moment mechanism. Do these differences imply that the details of the short range potential are liquid crystal dependent? We shall attempt to answer this question below.

To proceed, it is useful to introduce a model for the short range potential, $U_{sr,i}(\Omega)$. It seems sensible to choose a model that provides a successful fit to the orientational order parameters measured for a range of rigid solutes in a zero efg nematic solvent [7, 13, 23]. However, the internal motions in 5CB add extra complexity to the problem. It does not help that literature values of E_{tg} for butane vary from 400 to 900 cal mol^{-1} [24, 31–37]. Because we wish to draw meaningful conclusions from our work, we shall investigate two different models for the short range potential in an attempt to come up with a comparison among mixtures that is independent, as far as possible, of the model chosen. Since no significant differences between the zero efg mixtures 55 per cent 1132/EBBA and 56·5 per cent 1132/EBBA are observed, only the zero efg mixtures 55 per cent 1132/EBBA and 70 per cent 5CB/EBBA shall be compared in the following sections.

5.2. *CZ model*

Van der Est *et al.* [6], introduced the short range potential, $U_{sr}(\Omega)$,

$$U_{sr}(\Omega) = \tfrac{1}{2}kC(\Omega)^2 \tag{7}$$

to calculate order parameters of small solutes in the zero efg mixture 55 per cent 1132/EBBA. In equation (7), C is the circumference of the solute projected on to a plane perpendicular to the director, and k, a model parameter, is a property of the liquid crystal. In this model, the liquid crystal is treated as an elastic continuum. The solute is described as a collection of van der Waals spheres.

The order parameters recalculated from a one parameter fit of k in equation (7) to

46 solutes of varying symmetry agree well with the experimental order parameters [13, 23]. However, if the fit is done for individual solutes, the parameter k is consistently smaller for larger solutes such as 2,4-hexadiyne, 1CB and 5CB than for smaller ones. Consequently, Zimmerman *et al.* [13], introduced an additional term into the short range potential, $U_{sr}(\Omega)$, which yielded an excellent and consistent fit for large as well as small solutes in the zero efg mixture 55 per cent 1132/EBBA. The modified short range potential is written

$$U_{sr}(\Omega) = \tfrac{1}{2}k_z C(\Omega)^2 + \tfrac{1}{2}k_{xy} Z(\Omega) C(\Omega), \tag{8}$$

where k_z and k_{xy} are the model parameters. If the solute is considered as a cylinder, then equation (8) has the form of an anisotropic surface interaction. $Z(\Omega)$ is the maximum length of the solute, described as a collection of van der Waals spheres, projected on to the director direction for solute orientation Ω. Equation (8) can be rewritten in terms of the model parameters k_z and ξ,

$$U_{sr}(\Omega) = \tfrac{1}{2}k_z C(\Omega)^2 + \tfrac{1}{2}k_z \xi Z(\Omega) C(\Omega), \tag{9}$$

where $\xi = k_{xy}/k_z$ is dimensionless. Calculations using equation (8) or (9) for the short range potential shall be referred to as CZ model calculations in this paper. In the notation CZ, the 'C' refers to the $C(\Omega)$ term in equations (8) and (9), and the 'Z' to the $Z(\Omega)$ term.

5.3. *CI model*

In an attempt to introduce a better model for the anisotropic short range interaction between the solute surface and the liquid crystal, Zimmerman *et al.* [23], suggested that the short range potential can be written

$$U_{sr}(\Omega) = \tfrac{1}{2}kC(\Omega)^2 + \tfrac{1}{2}k_s \int C_Z(\Omega)\, dZ, \tag{10}$$

where k and k_s are the model parameters, and $C_Z(\Omega)$ is the circumference of the solute at distance Z. The second term in equation (10) models an anisotropic interaction between the solute surface and the liquid crystal. The first term, as in the case of van der Est *et al.* [6], accounts for the elastic distortion of the liquid crystal. This model gave the best fit to the experimental order parameters of 46 solutes in 55 per cent 1132/EBBA. Equation (10) can be rewritten in terms of the model parameters k_s and ξ' as

$$U_{sr}(\Omega) = \tfrac{1}{2}k_s \xi' C(\Omega)^2 + \tfrac{1}{2}k_s \int C_Z(\Omega)\, dZ, \tag{11}$$

where $\xi' = k/k_s$ is dimensionless. The calculations using equation (10) or (11) for the short range potential shall be referred to in this paper as CI model calculations. In the notation CI, the 'C' refers to the $C(\Omega)$ term in equations (10 and (11), and the 'I' to the integral term.

5.4. *RIS parameter and molecular geometry*

One of the complexities of the 5CB-d_{19} molecule is the presence of the flexible hydrocarbon chain which introduces the additional parameter, E_{tg}, the *trans–gauche* energy difference. Since E_{tg} is an intramolecular property, it should be independent of temperature and environment. E_{tg} values have been measured for *n*-butane in isotropic solvents and it would seem reasonable to use these values for 5CB-d_{19} in zero efg mixtures. Most of the literature values of liquid *n*-butane are close to 500 cal mol^{-1}

[33–36]. However, one study [32] reports a value of 966 cal mol^{-1} for gaseous *n*-butane. Since there are a range of E_{tg} values in the literature, we shall explore calculations using E_{tg} values of 500, 700 and 900 cal mol^{-1}.

In addition, the geometry of 5CB-d_{19} must be known in order to calculate the quadrupolar splittings. The parameters C and Z in the equations for $U_{sr}(\Omega)$ depend on the bond lengths, and the quadrupolar splittings depend on the bond angles. We assume that the benzene rings are regular hexagonal, and that the angle between the normals to the two benzene rings is 30° [17]. In addition, we assume that all the methylene groups are described by the CCC and CCD bond angles 112·5° and 108·82°. The DCD plane in each CD_2 group is assumed to bisect the CCC angle. The dihedral angle for a *trans–gauche* conformational change is 112·0°.

Two additional unknowns in the molecular geometry of 5CB-d_{19} are the angles θ' (see figure 1) and θ_d, where θ_d is the dihedral angle between the C_1C_2 bond and the plane of benzene ring *A*. Most studies of 5CB assume that the angle θ' is 120°. However, Photinos *et al.* [15], used the value 124° from X-ray studies on 5OCB for their calculations of *n*CB and *n*OCB liquid crystals. While 5OCB and 5CB will have different geometries, it nevertheless seems worthwhile to explore the possibility of a value of θ' different from 120° for 5CB. Of the many possibilities, we performed four different calculations corresponding to four different geometries: the four geometries are (1) $\theta' = 120°$, $\theta_d = 0°$ (the bond C_1C_2 is coplanar to the benzene ring *A*—this geometry shall be referred to as PL-0; (2) $\theta' = 124°$, $\theta_d = 0°$ (this geometry shall be referred to as PL-4); (3) $\theta' = 120°$, $\theta_d = 90°$ (the ring–C_1 bond lies along the *para*-axis of ring *A* and the bond C_1C_2 is perpendicular to the benzene ring *A*—this geometry shall be referred to as PERP-0); (4) $\theta' = 124°$, $\theta_d = 90°$ (starting from the PL-4 geometry, the hydrocarbon chain is rotated 90° about the *para*-axis of ring *A*—this geometry shall be referred to as PERP-4).

5.5. *Individual fit model parameters*

A least squares minimization routine was used to obtain best fit model parameters for each experimental spectrum from a minimization of the differences between experimental and calculated quadrupolar splittings of 5CB-d_{19} as solute in the zero efg

Table 4. Fitted ranges for θ of 5CB (see figure 1) in 55 per cent 1132/EBBA and 70 per cent 5CB/EBBA.

Model and geometry	E_{tg}/cal mol^{-1}	θ/deg of 55 per cent 1132/EBBA	θ/deg of 70 per cent 5CB/EBBA
COZ	500	118·88–117·48	118·70–117·48
	700	118·96–117·90	118·80–118·00
PERP-0	900	119·02–118·28	118·90–118·44
COZ	500	119·00–117·48	118·80–117·48
	700	119·14–118·04	118·96–118·18
PERP-4	900	119·26–118·58	119·14–118·78
CAI	500	119·76–122·20	119·94–122·68
	700	119·60–121·00	119·72–121·06
PERP-0	900	119·38–119·52	119·42–119·00
CAI	500	120·38–123·26	120·62–123·82
	700	120·18–121·88	120·34–122·00
PERP-4	900	119·88–120·12	119·90–120·04

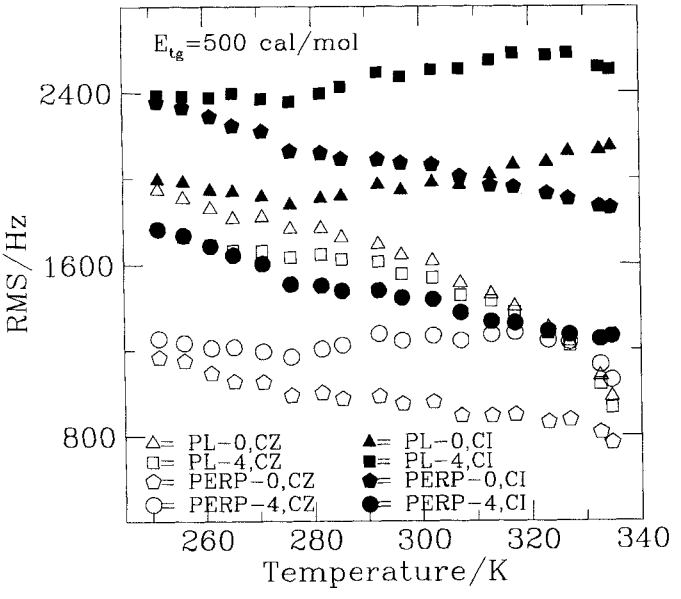

(*a*)

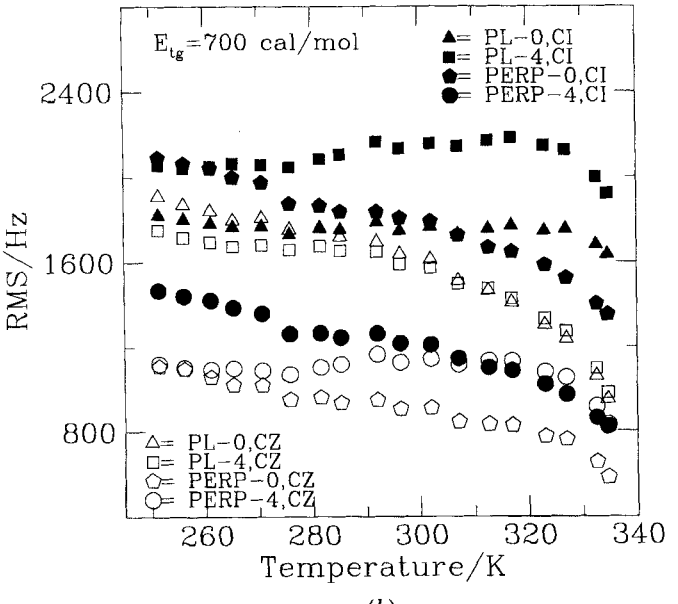

(*b*)

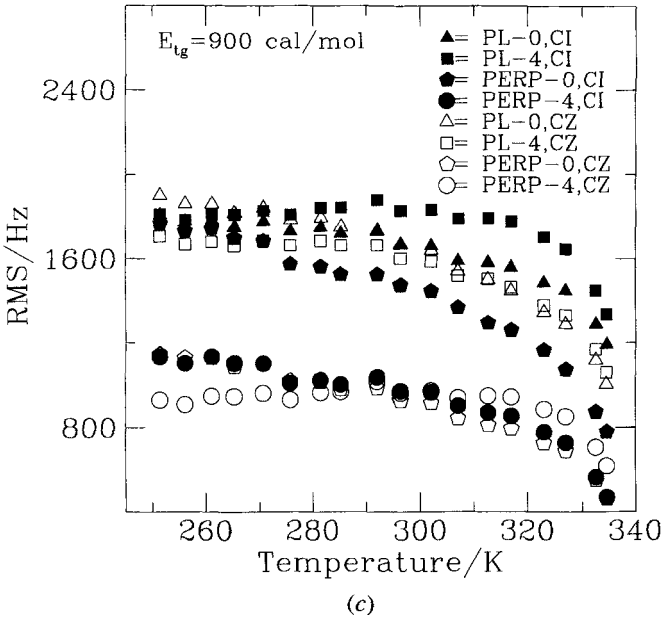

Figure 5. (*a*) RMS (root mean squares deviation) versus temperature of the fits to individual spectra of 5CB in 55 per cent 1132/EBBA for the different geometries PL-0, PL-4, PERP-0 and PERP-4. Open symbols are used for the CZ model with E_{tg} equal to 500 cal mol^{-1}. Closed symbols are used for the CI model with E_{tg} equal to 500 cal mol^{-1}. (*b*) the same as (*a*) for E_{tg} = 700 cal mol^{-1}. (*c*) the same as (*a*) for E_{tg} = 900 cal mol^{-1}.

mixtures 55 per cent 1132/EBBA and 70 per cent 5CB/EBBA. The quality of the fit is judged mainly from RMS (root mean square deviation) values, i.e. the lower the RMS the better the quality of the fit. We find that the quality of the fit depends on the parameters θ (see figure 1) and E_{tg}. When the angle θ was varied, the calculated quadrupolar splittings agreed very well with the experimental quadrupolar splittings at the ring positions. However, the variation of θ did not change much the calculated quadrupolar splittings at the chain positions. Hoatson *et al.* [12], also allowed θ to vary and obtained a good fit for the ring deuterons in their study of 5CB-d_{19} in liquid crystals. When the parameter E_{tg} was varied for each individual temperature, the best fit was obtained for E_{tg} values as low as 500 cal mol^{-1}. However, the fitted E_{tg} values varied with temperature. This contradicts the fact that the intramolecular property E_{tg} should be independent of temperature. Therefore, we decided to fix the parameter E_{tg} to certain values, 500, 700 and 900 cal mol^{-1}, at all temperatures. These values span the range of literature E_{tg} values [24, 31–37].

Separate calculations were performed for both the CZ and CI models for the four geometries PL-0, PL-4, PERP-0 and PERP-4 and for the three E_{tg} values 500, 700 and 900 cal mol^{-1}. The model parameters k_z, k_{xy} and θ were fitted in the CZ model calculations. The CI model calculation gives k, k_s and θ values. Therefore, we obtain 12 sets of (k_z, k_{xy}, θ) and of (k, k_s, θ) values for each spectrum. The fitted θ value ranges are reported in table 4. The θ values obtained are consistent with the value reported in [29]. In order to reduce the number of possible calculations in the following, we shall examine the quality of these fits and choose one set of k_z, k_{xy} and one set of k, k_s values. We shall choose the geometry and E_{tg} values that fit best the experimental quadrupolar

splittings as the most appropriate basis for comparison of the real intermolecular potential between mixtures.

The quality of the fit (RMS) to the 55 per cent 1132/EBBA mixture for the four different geometries using the two different models and three different E_{tg} values is shown in figure 5. While some fits are obviously much better than others, most of these fits are acceptable considering the many assumptions involved in the modelling process. It is unfortunate that the parameters are correlated such that it is not possible to choose a definitive value of E_{tg} from these calculations. However, calculations that use a value of E_{tg} of the order 500 cal mol^{-1} are generally considered preferable [15]. In all cases for the CI model, the PERP-4 geometry gives the best fit. For the CZ model, the PERP-0 geometry gives the best fit except for E_{tg} of 900 cal mol^{-1} at low temperatures, where the PERP-4 geometry gives the best fit. Similar results were obtained for the 70 per cent 5CB/EBBA mixture. Based of these plots, we decided to choose the PERP-0 geometry for the CZ model and the PERP-4 geometry for the CI model. Henceforth, whenever we refer to CZ model parameters, it implies that the parameters are calculated with the CZ model using the PERP-0 geometry. Similarly, any reference to the CI model parameters implies that the parameters are calculated with the CI model using the PERP-4 geometry.

5.5.1. *Temperature dependence of individual fit model parameters*

The temperature dependence of the short page potential is described by the temperature dependence of the CZ and CI model parameters. We use the parameters k_z and k_s to characterize the magnitude of the short range potentials. The parameters ξ and ξ' are ratios of model parameters. If all contributions to the potential scale the same way with temperature, these ratios would be independent of temperature. First, we shall analyse the temperature dependence of the model parameters k_z and k_s. Then, we shall examine the temperature dependence of the ratios ξ and ξ'.

5.5.2. k_z *and* k_s

Our main interest here is to see how the model parameters k_z and k_s depend on factors such as liquid crystal mixture, E_{tg} and temperature. The fitted k_z and k_s values obtained for each experimental temperature and for E_{tg} of 500, 700 and 900 cal mol^{-1} are plotted as reduced model parameters, k_i/T, against reduced temperature, $T_r = T/T_{NI}$, in figure 6. We use reduced model parameters because in the calculation of quadrupolar splittings the k_i are always divided by temperature; we use reduced temperature because the liquid crystal mixtures 55 per cent 1132/EBBA and 70 per cent 5CB/EBBA have different T_{NI} values.

As temperature increases towards T_{NI}, the reduced model parameters decrease. The k_z/T values of 55 per cent 1132/EBBA are higher than those of 70 per cent 5CB/EBBA at reduced temperatures less than 0·95, and this is true for all three E_{tg} values. The k_s/T values are quite similar in both mixtures. However, the break observed in figure 3 for the 70 per cent 5CB/EBBA mixture is also apparent in figure 6.

5.5.3. ξ *and* ξ'

The ratios ξ and ξ' are plotted against reduced temperature in figure 7. The similar results obtained for both samples, independent of model used, is striking. Thus the form of the short range potential appears to be the same in both mixtures.

The temperature dependence of ξ depends on E_{tg}. The ratio ξ has a large temperature dependence for the E_{tg} value 500 cal mol^{-1}, is less dependent on temperature for the

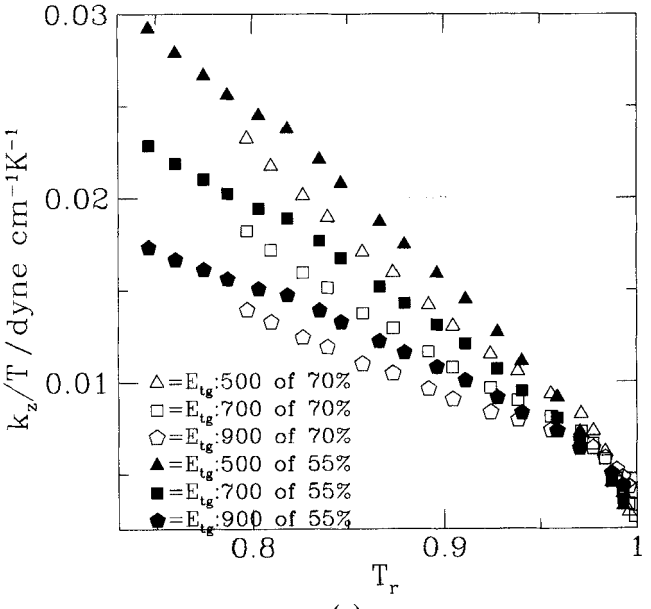

(*a*)

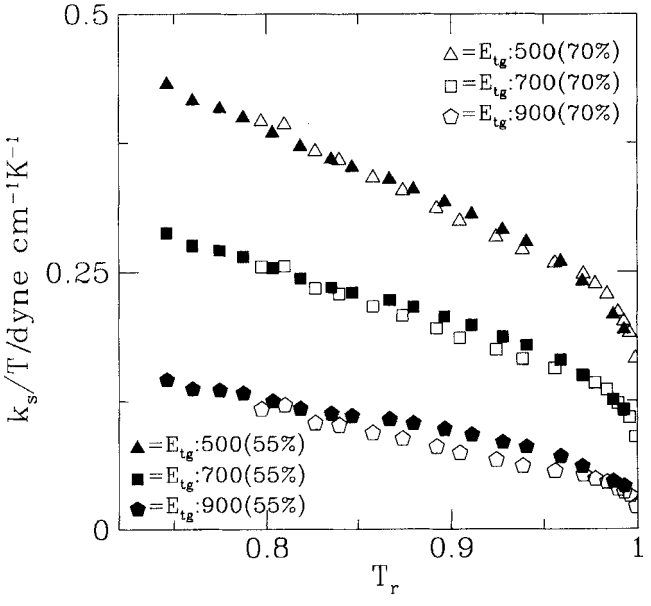

(*b*)

Figure 6. (*a*) The reduced model parameter k_z/T (CZ model, PERP-0 geometry) versus reduced temperature. Different symbols represent the k_z/T values of 70 per cent 5CB/EBBA (open symbols) and 55 per cent 1132/EBBA (filled symbols) for different E_{tg} values as indicated. (*b*) the reduced model parameter k_s/T (CI model, PERP-4 geometry) versus reduced temperature. The symbols have the same meaning as in (*a*).

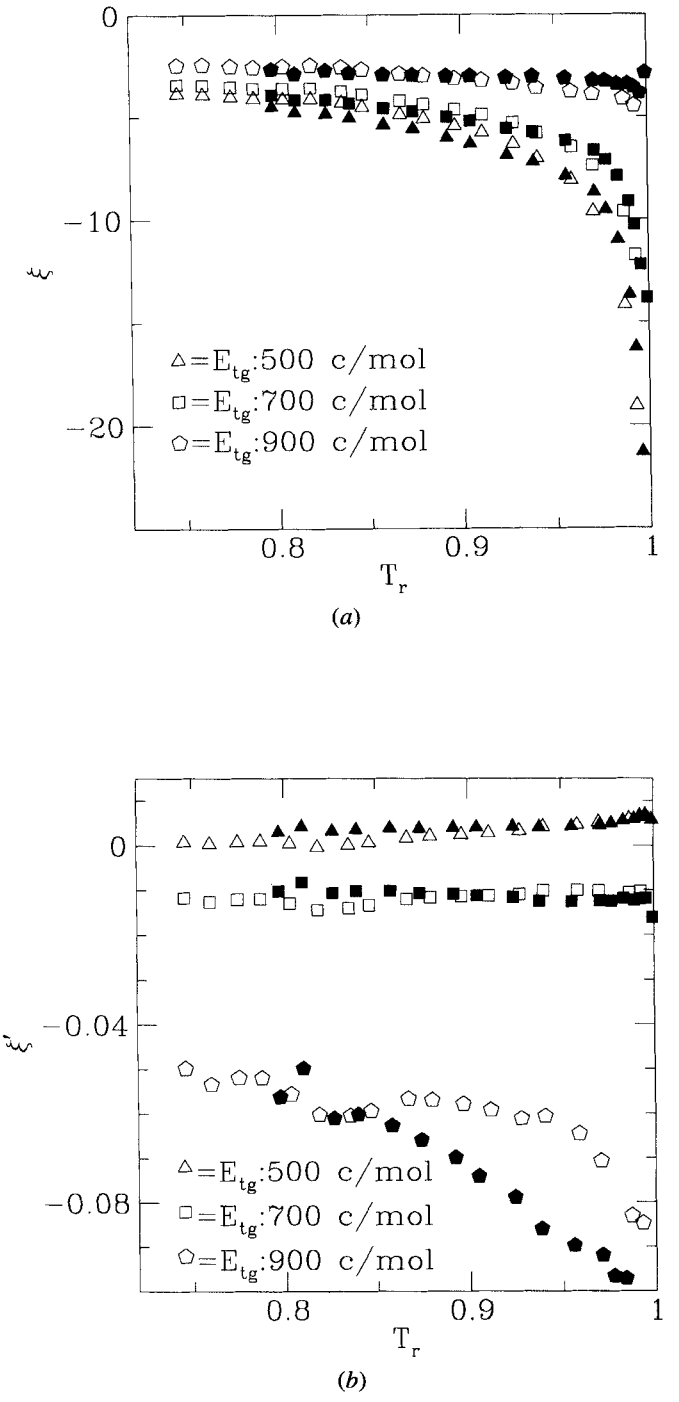

Figure 7. (*a*) The ratio ξ (CZ model, PERP-0 geometry) versus reduced temperature for 5CB Different symbols represent the ξ values of 70 per cent 5CB/EBBA (open symbols) and 55 per cent 1132/EBBA (filled symbols) for different E_{tg} values as indicated. (*b*) Ratio ξ' (CI model, PERP-4 geometry) versus reduced temperature. The symbols have the same meaning as in (*a*).

E_{tg} value 700 cal mol^{-1}, and is almost independent of temperature for the E_{tg} value 900 cal mol^{-1}. On the other hand, the ratio ξ' is small and has no significant temperature dependence for all E_{tg} values. Except for the CZ calculations at 500 and 700 cal mol^{-1}, these results are consistent with all terms in the potential having the same temperature dependence.

The small value of ξ' suggests that using only the second term of equation (10) or (11) would provide an excellent fit to the experimental results. It is precisely this term that provides the best one parameter fit to a collection of 46 solutes in the 55 per cent 1132/EBBA mixture [23].

5.6. *Global fit*

In §5.5, we have seen that the ratio ξ is independent of temperature for E_{tg} values close to 900 cal mol^{-1}, and ξ' is independent of temperature for E_{tg} values of 500 to 900 cal mol^{-1}. Constant values of ξ and ξ' are consistent with the reasonable guess that all contributions to the short range anisotropic potential have similar temperature dependence. In such a case, it is possible to calculate the parameters ξ and ξ' in a single least squares fit to all the experimental quadrupolar splittings at all temperatures for a given liquid crystal mixture. In addition, it is possible to determine the E_{tg} value in the same fit, since E_{tg} is independent of temperature. To reduce the number of adjustable parameters in such a fit, it is useful to choose some functional form for the temperature dependence of k_z and k_s. The variations of k_z and k_s from the individual fits to each temperature above resemble parabolas. To an excellent approximation, these k_z and k_s can be approximated by

$$k_i = k_0 + k_1 * (1 - T_r) + k_2 * (1 - T_r)^{1/2}. \tag{12}$$

Using this functional form in a fit to all experiments for a given sample at all temperatures gives the fitted parameters k_0, k_1 and k_2, ξ (or ξ'), E_{tg} and θ in table 5 for the CZ model and in table 6 for the CI model.

5.6.1. *Global fit model parameters*

It is instructive to compare the fitted parameters k_z (k_s), ξ (ξ') and E_{tg} to those from previous studies. First, we compare the parameters (k_z, ξ) and (k_s, ξ') to the values obtained from a study of 46 solutes in 55 per cent 1132/EBBA at 301 K [23]. The k_z value for the 55 per cent 1132/EBBA at 301 K in our study is 3·13 dyn cm^{-1}, which is close to the value 4·00 dyn cm^{-1} found in the study of 46 solutes in 55 per cent 1132/EBBA at 301 K [23]. However, the ratio ξ is $-2{\cdot}20$ in our study and $-3{\cdot}9$ for the 46 solutes [23]. Although the k_z values in these two studies are close, the ratio ξ in our study is much smaller than that for the 46 solutes [23]. Similarly, the fitted k and k_s values are 2·22 and 6·08 in our study compared to 2·04 and 48·0 for the 46 solutes in 55 per cent 1132/EBBA at 301 K [23].

Next, we compare the fitted E_{tg} values to those in the literature. The fitted E_{tg} values for 55 per cent 1132/EBBA are 952 and 1001 cal mol^{-1} and those for 70 per cent 5CB/EBBA are 911 and 972 cal mol^{-1} using the CZ (see table 5) and CI (see table 6) models. These E_{tg} values are high compared to most accepted literature values [24, 33–36] which are close to 500 cal mol^{-1}. However, we note that one study reports the value 966 cal mol^{-1} for E_{tg} of gaseous *n*-butane [32].

Since the fitted E_{tg} values are high compared to commonly accepted literature values (400–700 cal mol^{-1}), we shall explore the possibility of using a more acceptable value. For this purpose, we consider the RMS plots given in figure 5. For the CI model, the

Table 5. Fitted parameters of the CZ model using the PERP-0 geometry and varying E_{tg}. For a given liquid crystal mixture, the fit is to all experimental quadrupolar splittings at all temperatures. The k_i describe the temperature dependence of the model parameter k_z according to equation (12).

Fitted parameters	55 per cent 1132/EBBA	70 per cent 5CB/EBBA
k_0/dyne cm^{-1}	0·94 ± 0·06	1·11 ± 0·03
k_1/dyne cm^{-1}	− 2·28 ± 1·04	− 1·05 ± 1·07
k_2/dyne cm^{-1}	7·47 ± 0·50	5·41 ± 0·38
ξ	− 2·20 ± 0·23	− 2·73 ± 0·32
E_{tg}/cal mol^{-1}	952 ± 19	911 ± 21
θ/deg	118·94 ± 0·03	118·74 ± 0·03
RMS/Hz	1089	968

Table 6. Fitted parameters of the CI model using the PERP-4 geometry and varying E_{tg}. For a given liquid crystal mixture, the fit is to all experimental quadrupolar splittings at all temperatures. The k_i describe the temperature dependence of the model parameter k_s according to equation (12).

Fitted parameters	55 per cent 1132/EBBA	70 per cent 5CB/EBBA
k_0/dyne cm^{-1}	− 5·34 ± 1·48	− 5·57 ± 2·00
k_1/dyne cm^{-1}	30·68 ± 8·27	18·63 ± 6·73
k_2/dyne cm^{-1}	− 35·13 ± 9·39	− 21·84 ± 7·71
ξ'	− 0·16 ± 0·05	− 0·19 ± 0·08
E_{tg}/cal mol^{-1}	1001 ± 23	972 ± 23
θ/deg	119·68 ± 0·05	119·58 ± 0·08
RMS/Hz	946	1006

E_{tg} value 700 cal mol^{-1} gives acceptable fits, although larger E_{tg} values give better fits. Moreover, ξ' is independent of temperature when E_{tg} takes the value 700 cal mol^{-1}. For the CZ model, the ratio ξ is independent of temperature for high E_{tg} values. However, the E_{tg} value 700 cal mol^{-1} gives acceptable fits, and the ratio ξ is less dependent on temperature than for E_{tg} of 500 cal mol^{-1}. As a result, we chose the E_{tg} value 700 cal mol^{-1}, which is also the upper limit of the acceptable E_{tg} range, and repeated the least squares minimization keeping the E_{tg} value fixed at 700 cal mol^{-1} and adjusting the parameters k_0, k_1, k_2, θ, and ξ or ξ'.

The fitted values of k_0, k_1, k_2, θ, and ξ or ξ' are reported in table 7 or table 8 for the E_{tg} value 700 cal mol^{-1}. The RMS deviation in these fits is larger than when E_{tg} was varied, but the fits are still quite acceptable. We again compare the fitted values with those from the study of 46 solutes in 55 per cent 1132/EBBA. The k_z and ξ values are 4·03 and − 4·02 in our study, whereas these values are 3·92 and − 5·01 in the study of 46 solutes [23]. This is excellent agreement. In addition, the fitted k and k_s values in our study are − 0·80 and 76·4 compared to 2·04 and 48·0 in [23]. However, the k_s value 76·4 dyn cm^{-1} is very close to the k_s value 76·7 dyn cm^{-1} [23] obtained for the 46 solutes when the short range potential, $U_{sr,i}(\Omega)$, is expressed only in terms of k_s (i.e. $k = 0$). This is consistent with the separate fits at each temperature of k and k_s, §5.5, where it was found that the k_s term dominates the potential.

Table 7. Fitted parameters of the CZ model using the PERP-0 geometry and fixing E_{tg} at 700 cal mol^{-1}. For a given liquid crystal mixture, the fit is to all experimental quadrupolar splittings at all temperatures. The k_i describe the temperature dependence of the model parameter k_z according to equation (12).

Fitted parameters	55 per cent 1132/EBBA	70 per cent 5CB/EBBA
k_0/dyne cm^{-1}	0·83 ± 0·12	1·08 ± 0·05
k_1/dyne cm^{-1}	1·66 ± 1·96	2·29 ± 1·30
k_2/dyne cm^{-1}	9·25 ± 1·07	6·39 ± 0·59
ξ	− 4·02 ± 0·11	− 4·79 ± 0·14
E_{tg}/cal mol^{-1}	700·00	700·00
θ/deg	119·38 ± 0·04	119·27 ± 0·04
RMS/Hz	1594	1405

Table 8. Fitted parameters of the CI model using the PERP-4 geometry and fixing E_{tg} at 700 cal mol^{-1}. For a given liquid crystal mixture, the fit is to all experimental quadrupolar splittings at all temperatures. The k_i describe the temperature dependence of the model parameter k_s according to equation (12).

Fitted parameters	55 per cent 1132/EBBA	70 per cent 5CB/EBBA
k_0/dyne cm^{-1}	− 25·27 ± 1·49	− 28·55 ± 1·28
k_1/dyne cm^{-1}	115·05 ± 16·67	78·05 ± 15·46
k_2/dyne cm^{-1}	− 147·87 ± 10·39	− 102·59 ± 8·15
ξ'	− 0·013 ± 0·002	− 0·013 ± 0·002
E_{tg}/cal mol^{-1}	700·00	700·00
θ/deg	120·50 ± 0·04	120·74 ± 0·06
RMS/Hz	1390	1464

5.7. *Comparison of short range interactions*

In equation (3) we note that all potential terms are divided by T. A simple Maier–Saupe mean field theory of nematics [38] would predict a unique value for $U_{sr\,i}(\Omega)/T$ at the nematic–isotropic phase transition temperature, T_{NI}. As T_{NI} varies for different liquid crystals, and as $U_{int,\,i}$ is a constant for a given conformer, the $U_{int,\,i}/T_{NI}$ part of the potential for the solute 5CB at the nematic–isotropic transition will vary inversely with T_{NI}. The simple Maier–Saupe potential predicts the same reduced temperature, $T_r = T/T_{NI}$, dependence of the order parameter. Thus differences at T_{NI} are expected to propagate throughout the nematic temperature range. Could this variation with T_{NI} of the $U_{int,\,i}/T$ part of the potential account for the observed spectral differences? To examine this possibility in terms of the intra- and inter-molecular potentials acting on 5CB as solute in the nematic mixtures that we are investigating here, we need to analyse the results in terms of the parameters on which these potentials, and thus the quadrupolar splittings, depend.

In §5.5 we saw that fits to the spectrum obtained at each individual temperature using the E_{tg} value 700 cal mol^{-1} give very good agreement between the experimental and calculated quadrupolar splittings. In §5.6 we found that the global fit calculation using the E_{tg} value 700 cal mol^{-1} gives very good agreement between the fitted model parameters in our study and the parameters found in a study of 46 solutes in the 55 per cent 1132/EBBA zero electric field gradient nematic mixture [13, 23]. Therefore, an appropriate choice of E_{tg} for comparison of the short range potentials in the zero electric field gradient mixtures is 700 cal mol^{-1}. The model parameters k_i are k_z and k_{xy} for the

CZ model, (equation (8)), and k and k_s for the CI model, (equation (10)). Therefore, the quadrupolar splitting of deuteron j, $\Delta\nu_j$, can be written

$$\Delta\nu_j = f\left(j, \frac{k_z}{T}, \frac{k_{xy}}{T}, \frac{E_{tg}}{T}\right) \tag{13}$$

for the CZ model with a similar equation for the CI model.

To compare the potentials in the various liquid crystals, it is instructive to plot the calculated k_i/T values versus $\Delta\nu_1$. The choice of $\Delta\nu_1$ as a plotting parameter requires some explanation. In the quadrupolar splitting versus temperature plot in figure 3 and the k_i/T versus reduced temperature plots in figure 6 an unusual temperature dependence was observed for the 70 per cent 5CB/EBBA mixture. Therefore we wish to choose a quantity, other than reduced temperature, for comparison. The first quantity that comes to mind is the order parameter for the sample. However, this quantity is difficult to define, especially for the liquid crystal mixtures used in this work. In addition, a Maier–Saupe mean field theory for binary mixtures of axially symmetric nematic liquid crystals gives the anisotropic part of the mean-field intermolecular potential for particle i as [39–41]

$$U_i(\Omega) = [\rho_i U_{ii} S_i + \rho_j U_{ij} S_j] P_2(\cos\Omega), \tag{14}$$

where ρ_i is the number density of component i, U_{ij} is the anisotropic interaction strength between components i and j, and S_i is the order parameter of component i. Note that it is easy to extend equation (14) to multicomponent mixtures by adding a U_{ij} term for each component. This potential predicts, in general, different values for the order parameters of components i and j. In addition the value of $U_i(\Omega)/T$ for a given liquid crystal i will not necessarily be the same at a given reduced temperature in different mixtures; this could explain some of the difference between mixtures observed in figure 6. As we wish to compare the intermolecular potential acting on our solute 5CB in the different liquid crystal mixtures, it would make sense to choose for comparison situations where the order parameter of the solute is the same. In terms of equation (14) for an axially symmetric nematic, this would require that $U_i(\Omega)/T$ be the same in both mixtures. In the real case, 5CB is not axially symmetric, and exists in many conformations. Thus the test for similar potentials would be that the various contributions to the potential, i.e. the two terms in equations (8) to (11) or the terms in equation (14), divided by temperature, give equal contributions to the total potential. Fortunately the lack of symmetry in 5CB allows us to fit our spectral results to potentials with more than one parameter: the comparison between mixtures than involves comparison of these parameters.

As an aside, equation (14) has also been used to describe mixtures of a nematic liquid crystal with a solute that does not itself exhibit a liquid crystalline phase [42]. Thus, for all solutes i to experience the same anisotropic potential in different liquid crystal mixtures, in terms of equation (14) it is required that $U_{ik} = c_{kj} \times U_{ij}$ with c_{kj} a constant depending only on liquid crystal components j and k, but being independent of solute i. Note that the requirement for a zero field gradient mixture is that for all solutes the anisotropic components of the field gradient cancel when terms for all component liquid crystals are added.

Because of the lack of symmetry and the intramolecular motions in 5CB, the choice of its order parameter for comparison purposes presents a problem. A more convenient choice would be the quadrupolar splittings $\Delta\nu_j$ of 5CB-d_{19} which are related to this order parameter. But which splitting is the best to use? Note that we are interested in

separating the temperature effects of the $U_{\text{int},i}$ and $U_{\text{sr}i}(\Omega)$. In a calculation of the quadrupolar splittings of 5CB-d_{19} at two different temperatures having the same k_i/T values, we found that the quadrupolar splitting $\Delta\nu_1$ is the least dependent upon the E_{tg}/T term. Thus it is appropriate to use $\Delta\nu_1$ for comparing the liquid crystal mixtures.

To examine the liquid crystal mixture dependence of the k_i parameters, we plot k_z/T, k_{xy}/T, k_s/T and k/T versus $\Delta\nu_1$ in figures 8–11. The k_i values in these plots are those that were obtained from a separate least squares fitting for each spectrum at each different temperature. The plots in these figures show that for a given $\Delta\nu_1$, the k_i/T values of 55 per cent 1132/EBBA are in excellent agreement with those of 70 per cent 5CB/EBBA. Based on this agreement, we can write for a given $\Delta\nu_1$

$$(k_i/T)_{55} = (k_i/T)_{70} \tag{15}$$

where k_i/T can be k_z/T, k_{xy}/T, k_s/T or k/T. The subscripts 55 and 70 stand for the liquid crystal mixtures 55 per cent 1132/EBBA and 70 per cent 5CB/EBBA. This demonstrates that the choice of $\Delta\nu_1$ (as a parameter proportional to the 5CB order parameter) for comparison purposes was a good one. Because the two parameters describing the potential scale in the same way, figures 8 to 11 demonstrate that the anisotropic short range potentials in 55 per cent 1132/EBBA and 70 per cent 5CB/EBBA are the same. Substituting equation (15) into equations (8) and (10), we obtain for a given $\Delta\nu_1$

$$(U_{\text{sr}}/T)_{55} = (U_{\text{sr}}/T)_{70}. \tag{16}$$

Thus, for a given $\Delta\nu_1$, the experimental results are described by the same reduced short range potentials and reduced model parameters for both zero electric field gradient mixtures. This conclusion is independent of the model chosen for analysis. Note that by a reduced quantity we mean the actual quantity divided by temperature.

As the purpose of this paper is to examine several zero electric field gradient mixtures and to investigate to what extent the description of the anisotropic short range potential is similar in the various mixtures, it is worthwhile analysing equations (15) and (16) further. As pointed out above, one way of emphasizing small differences among zero electric field gradient mixtures is to plot ratios of the quadrupolar splittings, such as $\Delta\nu_5/\Delta\nu_1$, against $\Delta\nu_1$. In figure 4 we chose the ratio $\Delta\nu_5/\Delta\nu_1$ for comparison, because the quadrupolar splittings at the 5-position are more difficult to fit than the quadrupolar splittings at other positions of the chain. This is because the methyl deuterons are sensitive to all internal chain motions. However, qualitatively similar results are obtained for other chain positions.

In figures 12 and 13 we compare experimental ratios from figure 4 (filled symbols) with those recalculated from the best-fit parameters obtained from separate fits to each experimental spectrum in §5.5 (dotted symbols). Figure 12 presents results for the CZ model, and figure 13 for the CI model. Although there is a deviation between the calculated and experimental quadrupolar splitting ratios, the general experimental trends are observed with both models. More important, the differences between the liquid crystal mixtures are well predicted. The deviation between experiment and theory is mainly due to the inadequacy of the models.

We now turn to the question 'If the intermolecular potential is the same, why do the quadrupolar splitting ratios $\Delta\nu_5/\Delta\nu_1$ differ with liquid crystal solvent in the ratio plots of figures 12 and 13?' Equation (13) tells us that there is another parameter, E_{tg}/T, on which the quadrupolar splitting $\Delta\nu_j$ depends. The value of E_{tg} is constant, and is set to 700 cal mol^{-1}. However, the temperature at which a given $\Delta\nu_1$ is observed in the 55

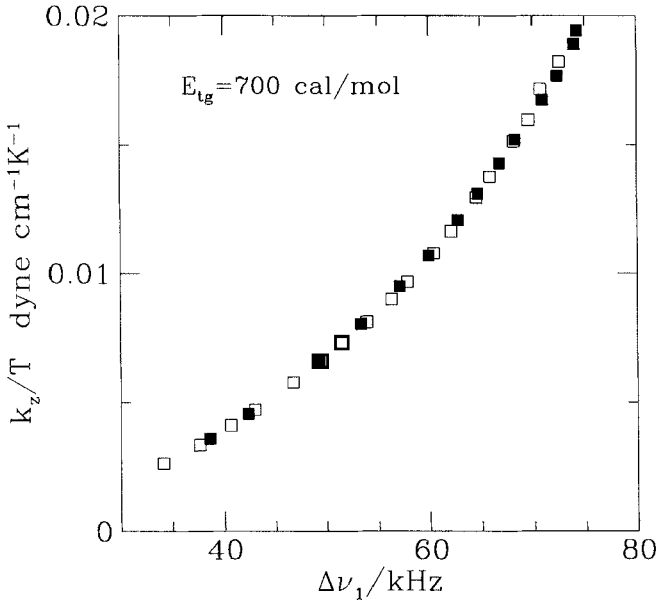

Figure 8. Reduced model parameter, k_z/T (CZ model, PERP-0 geometry), against quadrupolar splitting $\Delta\nu_1$ for the E_{tg} value 700 cal mol^{-1}. Open squares (□) 70 per cent 5CB/EBBA. Closed squares (■) 55 per cent 1132/EBBA.

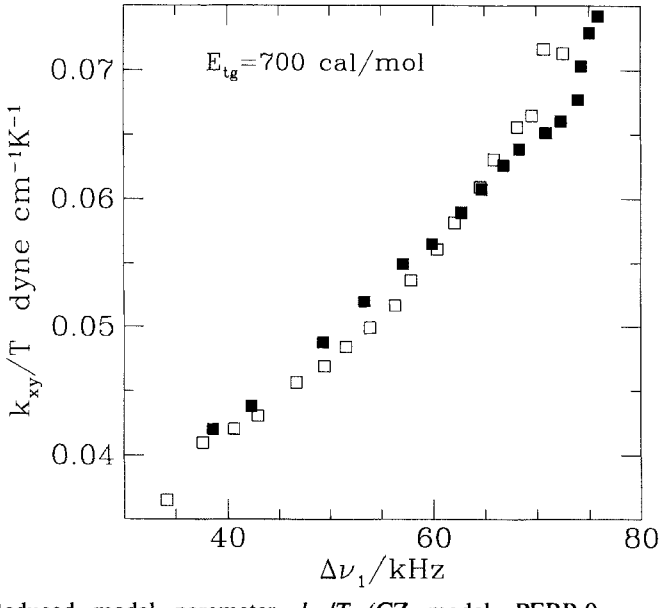

Figure 9. Reduced model parameter, k_{xy}/T (CZ model, PERP-0 geometry), against quadrupolar splitting $\Delta\nu_1$ for the E_{tg} value 700 cal mol^{-1}. Open squares (□) 70 per cent 5CB/EBBA. Closed squares (■) 55 per cent 1132/EBBA.

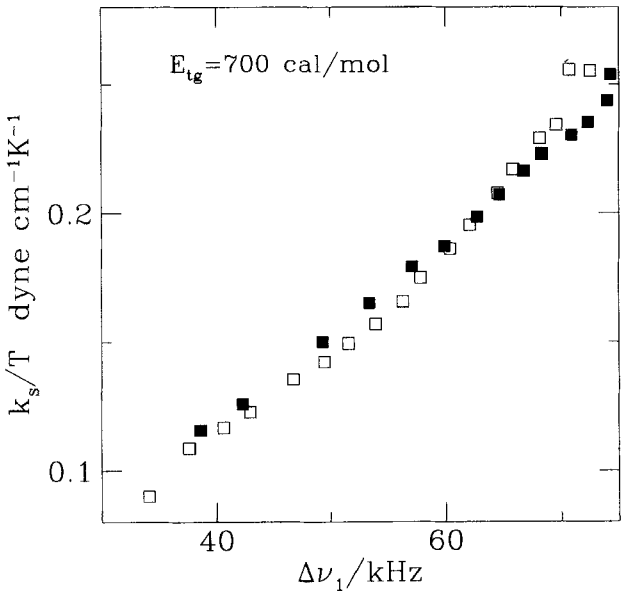

Figure 10. Reduced model parameter, k_s/T (CI model, PERP-4 geometry), against quadrupolar splitting $\Delta\nu_1$ for the E_{tg} value 700 cal mol^{-1}. Open squares (□) 70 per cent 5CB/EBBA. Closed squares (■) 55 per cent 1132/EBBA.

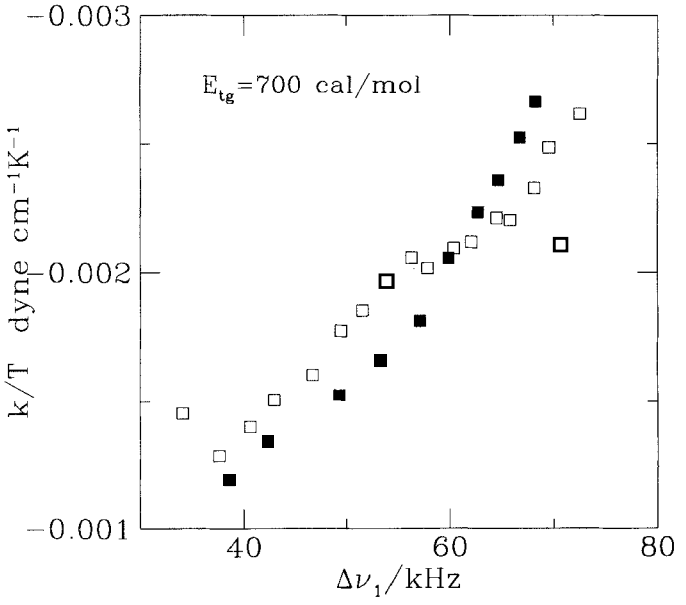

Figure 11. Reduced model parameter, k/T (CI model, PERP-4 geometry), against quadrupolar splitting $\Delta\nu_1$ for the E_{tg} value 700 cal mol^{-1}. Open squares (□) 70 per cent 5CB/EBBA. Closed squares (■) 55 per cent 1132/EBBA.

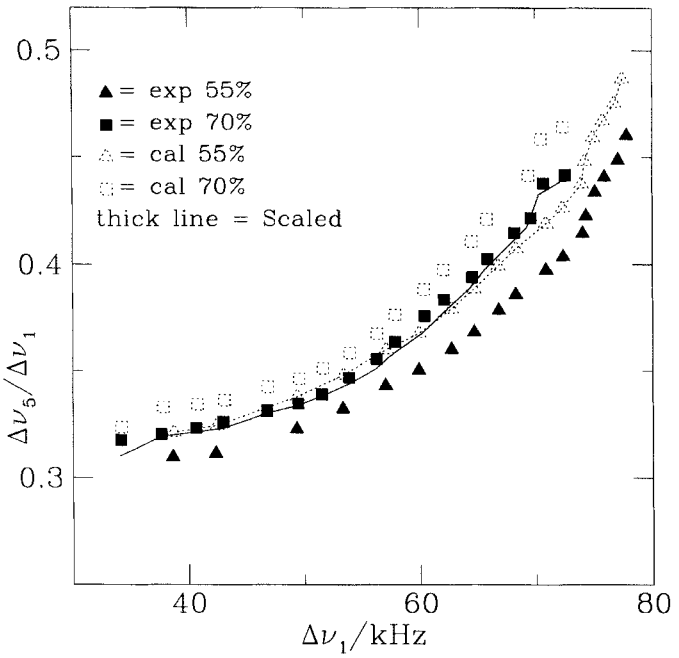

Figure 12. Quadrupolar splitting ratios $\Delta\nu_5/\Delta\nu_1$ versus $\Delta\nu_1$ (CZ model, PERP-0 geometry). Individual fit CZ model parameters were used to calculate the recalculated (dotted symbols and line) and 'scaled' (solid line) quadrupolar splitting ratios.

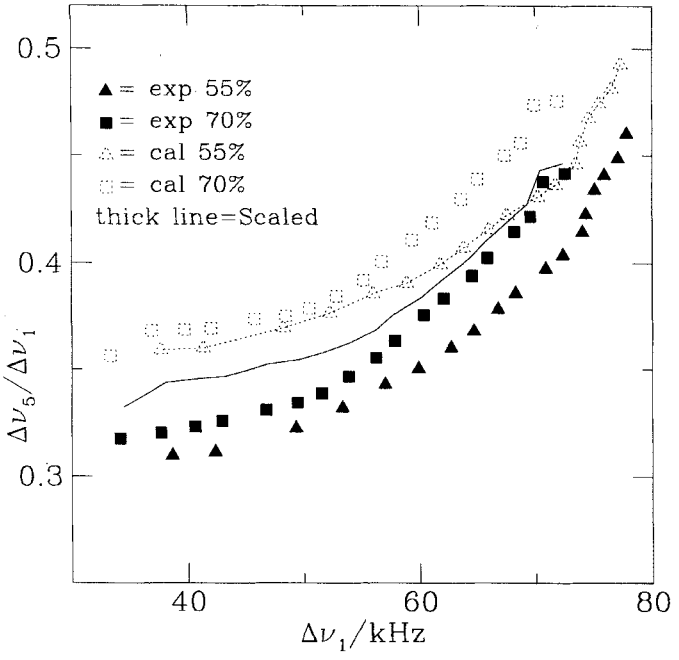

Figure 13. Quadrupolar splitting ratios $\Delta\nu_5/\Delta\nu_1$ versus $\Delta\nu_1$ (CI model, PERP-4 geometry). Individual fit CI model parameters were used to calculate the recalculated (dotted symbols and line) and 'scaled' (solid line) quadrupolar splitting ratios.

Table 9. Temperature scaling factors, TSF (see text).

T_{70}/K of 70 per cent 5CB/EBBA	TSF	T_{70}/K of 70 per cent 5CB/EBBA	TSF
251·9	1·114	296·6	1·077
255·9	1·117	302·0	1·069
261·2	1·107	306·8	1·061
265·3	1·108	308·8	1·058
271·1	1·106	310·8	1·058
276·1	1·097	312·7	1·062
281·9	1·094	313·7	1·061
285·9	1·092	314·7	1·065
292·1	1·082	315·7	1·065
		$TSF_{average}$	1·083

per cent 1132/EBBA mixture, T_{55}, is different from that in the 70 per cent 5CB/EBBA mixture, T_{70}. As a result, the E_{tg}/T term is different for the two mixtures. Therefore, the differences in quadrupolar splitting ratios $\Delta\nu_5/\Delta\nu_1$ must be due to the different temperatures (T_{55} and T_{70}) associated with the different liquid crystal mixtures 55 per cent 1132/EBBA and 70 per cent 5CB/EBBA.

Of course, the above analysis is based on independent fits of spectra in the different mixtures. Perhaps a better demonstration that the spectral differences are due to the temperature dependence of the conformational averaging would be to predict the spectrum of one mixture from the k_i parameters of the other mixture. We shall call the quadrupolar splittings of these predicted spectra 'scaled quadrupolar splittings'.

In this study, we shall start from the reduced model parameters of 70 per cent 5CB/EBBA and shall predict the quadrupolar splittings of the 55 per cent 1132/EBBA mixture. In order to predict the quadrupolar splittings in 55 per cent 1132/EBBA, it is necessary to use the appropriate temperatures in the E_{tg}/T term; the temperature in the E_{tg}/T term has to be scaled by a factor T_{55}/T_{70}. In order to simplify the notation, we define this factor T_{55}/T_{70} as the temperature scaling factor (TSF). The TSF values are calculated from the results for a given $\Delta\nu_1$ and tabulated with the corresponding temperatures of the 70 per cent 5CB/EBBA mixture in table 9. For each entry in table 9, the reduced short range potentials $U_{sr,i}(\Omega)/T$ along with $U_{int,i}/(T_{70} \times \text{TSF})$ are used to calculate the 'scaled quadrupolar splittings'. If we are correct that the spectral differences arise from the temperature effect on the conformational averaging, these scaled splittings should equal the recalculated splittings of 5CB-d_{19} in the 55 per cent 1132/EBBA mixture. To demonstrate that this is indeed the case, we plot 'scaled' along with experimental and recalculated quadrupolar splitting ratios $\Delta\nu_5/\Delta\nu_1$ in figure 12 (CZ model) and 13 (CI model). The agreement between the 'scaled' (thick lines, predicted from the results of the 70 per cent 5CB/EBBA experiments) and recalculated (dotted lines, fits to the 55 per cent 1132/EBBA experiments themselves) quadrupolar splitting ratios is excellent for the CZ model. This agreement confirms that the differences in the quadrupolar splitting ratios $\Delta\nu_5/\Delta\nu_1$ come from the different temperatures T_{55} and T_{70} of 55 per cent 1132/EBBA and 70 per cent 5CB/EBBA for a given $\Delta\nu_1$. For a given value of $U_{sr,i}(\Omega)/T$, the different temperatures affect the quadrupolar splittings via the effect of the different $U_{int,i}/T$ on the conformational averaging.

In §5.6 the results were analysed by fitting all spectra at all temperatures in a given liquid crystal solvent to a set of global parameters. In these fits the ratio between the k_i values, ξ or ξ', were kept constant for a given solvent. Above we have seen that, for

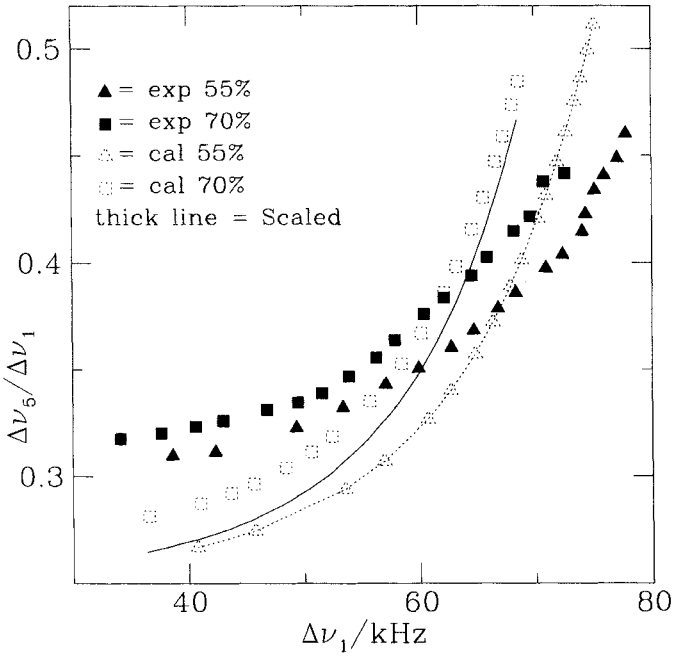

Figure 14. Quadrupolar splitting ratios $\Delta\nu_5/\Delta\nu_1$ versus $\Delta\nu_1$ (CZ model, PERP-0 geometry). Global fit CZ model parameters were used to calculate the recalculated (dotted symbols and line) and 'scaled' (solid line) quadrupolar splitting ratios.

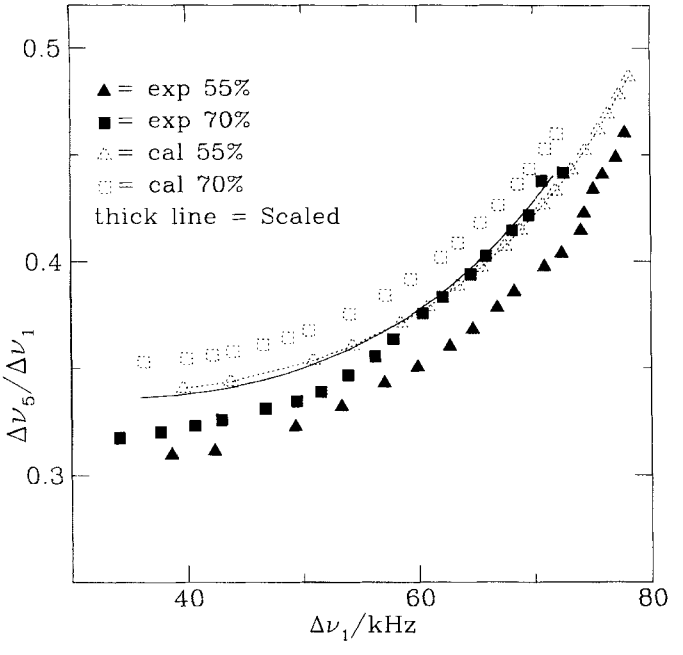

Figure 15. Quadrupolar splitting ratios $\Delta\nu_5/\Delta\nu_1$ versus $\Delta\nu_1$ (CI model, PERP-4 geometry). Global fit CI model parameters were used to calculate the recalculated (dotted symbols and line) and 'scaled' (solid line) quadrupolar splitting ratios.

a given experimental $\Delta\nu_1$, the reduced model parameters are transferable from one zero electric field gradient mixture to another and the reduced short range potentials of the two zero electric field gradient mixtures are equal. The global fit parameters can be tested in a similar analysis.

First, we shall examine the fitted parameters in tables 7 and 8 corresponding to E_{tg} of 700 cal mol^{-1}. Based on equation (15), we intuitively expect that the ratios $\xi = k_{xy}/k_z$ or $\xi' = k/k_s$ should be the same in all zero electric field gradient mixtures. The ξ values are $-4{\cdot}02$ and $-4{\cdot}79$ and the ξ' values are $-0{\cdot}013$ and $-0{\cdot}013$ for the liquid crystal mixtures 55 per cent 1132/EBBA and 70 per cent 5CB/EBBA. The ξ and ξ' values of these two liquid crystal mixtures are in excellent agreement. Thus, the ratios ξ and ξ' are transferable from one zero electric field gradient mixture to another.

As was the situation above, a most useful comparison is to check the transferability of reduced model parameters by calculating the 'scaled quadrupolar splittings'. We start with the reduced model parameters k_0/T_{70}, k_1/T_{70} and k_2/T_{70} of 70 per cent 5CB/EBBA. Then we use $T = T_{70} \times \mathrm{TSF}_{\mathrm{average}}$ (see table 9) in the calculation of $U_{\mathrm{int},i}/T$ to calculate the 'scaled quadrupolar splittings'.

The 'scaled', experimental and recalculated quadrupolar splitting ratios $\Delta\nu_5/\Delta\nu_1$ are plotted against $\Delta\nu_1$ in figure 14 (CZ model) and 15 (CI model. The agreement between the 'scaled' (solid line, predicted from the results of the 70 per cent 5CB/EBBA experiments) and recalculated (dotted line, fits to the 55 per cent 1132/EBBA experiments themselves) quadrupolar splitting ratios is excellent for the CI model. In addition, the fits are in reasonable agreement with the experimental results, and the general features of the experimental quadrupolar splittings are predicted. In this case a temperature independent ξ' seems the correct choice. For the CZ model, however, the fits are not as good. This is because the ξ parameter was kept constant with temperature. Above it was shown for this model with $E_{tg} \leq 700$ cal mol^{-1} that the best results are obtained with a temperature dependent ξ. This is evident from the deviation between the experimental and recalculated quadrupolar splitting ratios in figure 14. The 'scaled quadrupolar splitting' ratios agree well with the recalculated quadrupolar splitting ratios at high temperatures. However, the deviation is large for low temperatures. This deviation is partly due to the fact that the TSF ratios, T_{55}/T_{70}, at low temperatures are very different from the $\mathrm{TSF}_{\mathrm{average}}$ (1·083) whereas these ratios are very close to the $\mathrm{TSF}_{\mathrm{average}}$ at high temperatures.

6. Conclusions

The quadrupolar splittings of 5CB-d_{19} in the zero efg mixtures 55 per cent 1132/EBBA and 56·5 per cent 1132/EBBA are almost equal at any given temperature. Therefore, the short range potentials in these two mixtures are the same. However, the quadrupolar splittings of 5CB-d_{19} in the zero efg mixture 70 per cent 5CB/EBBA are different from those of 55 per cent 1132/EBBA at any given temperature. These differences at a given temperature are due to the different magnitudes of the short range potentials in these mixtures. The CZ and CI models describing the short range potentials are both successful in calculating the quadrupolar splittings of 5CB-d_{19} in the mixtures 55 per cent 1132/EBBA and 70 per cent 5CB/EBBA. In both cases the *trans–gauche* energy difference is consistent with the upper range of acceptable values, 700 kcal mol^{-1}. The model parameters k_z and k_{xy} of the CZ model and k and k_s of the CI model are useful in comparing the short range potentials between these two mixtures. The values obtained agree quite well with those obtained from a study of 46 solutes in a zero efg nematic solvent.

In this paper we have demonstrated in several different ways that for a given experimental $\Delta\nu_1$ the reduced model parameters k_i/T of 55 per cent 1132/EBBA are the same as those of 70 per cent 5CB/EBBA. That is, irrespective of the model used for analysis, the reduced short range potential appears to be the same in all zero electric field gradient nematic mixtures. In other words, the quadrupolar splittings of 5CB-d_{19} in one zero electric field gradient mixture can be predicted knowing the reduced model parameters of another zero electric field gradient mixture. The differences in spectra between mixtures, and in ratio plots such as those of figure 4, result from the temperature dependence of the internal energy contribution to the conformer probabilities.

We thank Dr Mary E. Neubert of The Liquid Crystal Institute, Kent State University for her assistance in determining the liquid crystal phase and the nematic–isotropic transition temperatures using microscopy. We also thank Leon ter Beek, James Polson and Z. Sun for their valuable discussions. We thank J. B. S. Barnhoorn of The Free University of Amsterdam for the gift of EBBA. We acknowledge the Natural Sciences and Engineering Research Council of Canada and The Petroleum Research Fund, administered by the ACS, for support of this research. We are grateful to the referee for the many helpful comments and criticisms of the original draft of this paper.

References

[1] SAUPE, A., 1966, *Molec. Cryst.*, **1,** 527.
[2] LUCKHURST, G. R., 1985, *Nuclear Magnetic Resonance of Liquid Crystals*, p. 53.
[3] COUNSELL, C. J., EMSLEY, J. W., HEATON, N. J., and LUCKHURST, G. R., 1984, *Molec. Phys.*, **54,** 847.
[4] DIEHL, P., and KHETRAPAL, C. L., 1969, *NMR Basic Principles and Progress*, Vol. 1 (Springer).
[5] EMSLEY, J. W., and LINDON, J. C., 1975, *NMR Spectroscopy Using Liquid Crystal Solvents* (Pergamon).
[6] VAN DER EST, A. J., KOK, M. Y., and BURNELL, E. E., 1987, *Molec. Phys.*, **60,** 397.
[7] VAN DER EST, A. J., 1987, Ph.D. thesis, University of British Columbia.
[8] BARKER, P. B., VAN DER EST, A. J., BURNELL, E. E., PATEY, G. N., DE LANGE, C. A., and SNIJDERS, J. G., 1984, *Chem. Phys. Lett.*, **107,** 426.
[9] PATEY, G. N., BURNELL, E. E., SNIJDERS, J. G., and DE LANGE, C. A., 1983, *Chem. Phys. Lett.*, **99,** 271.
[10] VAN DER EST, A. J., BARKER, P. B., BURNELL, E. E., DE LANGE, C. A., and SNIJDERS, J. G., 1985, *Molec. Phys.*, **56,** 161.
[11] BAILEY, A. L., BATES, G. S., BURNELL, E. E., and HOATSON, G. L., 1989, *Liq. Crystals*, **5,** 941.
[12] HOATSON, G. L., BAILEY, A. L., VAN DER EST, A. J., BATES, G. S., and BURNELL, E. E., 1988, *Liq. Crystals*, **3,** 683.
[13] ZIMMERMAN, D. S., and BURNELL, E. E., 1990, *Molec. Phys.*, **69,** 1059.
[14] BARNHOORN, J. B. S., DE LANGE, C. A., and BURNELL, E. E., 1993, *Liq. Crystals*, **13,** 319.
[15] PHOTINOS, D. J., SAMULSKI, E. T., and TORIUMI, H., 1991, *J. chem. Phys.*, **94,** 2758.
[16] SAMULSKI, E. T., and DONG, R. Y., 1982, *J. chem. Phys.*, **77,** 5090.
[17] SINTON, S. W., ZAX, D. B., MURDOCH, J. B., and PINES, A., 1984, *Molec. Phys.*, **53,** 333.
[18] EMSLEY, J. W., LUCKHURST, G. R., GRAY, G. W., and MOSLEY, A., 1978, *Molec. Phys.*, **35,** 1499.
[19] EMSLEY, J. W., LINDON, J. C., and LUCKHURST, G. R., 1975, *Molec. Phys.*, **30,** 1913.
[20] SINTON, S. W., and PINES, A., 1980, *Chem. Phys. Lett.*, **76,** 263.
[21] EMSLEY, J. W., LUCKHURST, G. R., and STOCKLEY, C. P., 1982, *Proc. R. Soc.* A, **381,** 117.
[22] WEAVER, A., VAN DER EST, A. J., RENDELL, J. C. T., HOATSON, G. L., BATES, G. S., and BURNELL, E. E., 1987, *Liq. Crystals*, **2,** 633.
[23] ZIMMERMAN, D. S., and BURNELL, E. E., 1993, *Molec. Phys.*, **78,** 687.
[24] FLORY, P. J., 1969, *Statistical Mechanics of Chain Molecules* (Wiley Interscience).

[25] EMSLEY, J. W., and LUCKHURST, G. R., 1980, *Molec. Phys.*, **41,** 19.
[26] BURNELL, E. E., DE LANGE, C. A., and MOURITSEN, O. G., 1982, *J. magn. Reson.*, **50,** 188.
[27] KELLER, P., and LIEBERT, L., 1978, *Solid St. Phys. Suppl.*, **14,** 19.
[28] DAVIS, J. H., JEFFREY, K. R., BLOOM, M., VALIC, M. I., and HIGGS, T. P., 1976, *Chem. Phys. Lett.*, **42,** 390.
[29] EMSLEY, J. W., LUCKHURST, G. R., and STOCKLEY, C. P., 1981, *Molec. Phys.*, **44,** 565.
[30] VAN DER EST, A. J., BURNELL, E. E., and LOUNILA, J., 1988, *J. chem. Soc. Faraday Trans. II*, **84,** 1095.
[31] SHEPPARD, N., and SZASZ, G. J., 1949, *J. chem. Phys.*, **17,** 86.
[32] VERMA, A. L., MURPHY, W. F., and BERNSTEIN, H. J., 1974, *J. chem. Phys.*, **60,** 1540.
[33] BRADFORD, W. F., FITZWATER, S., and BARTELL, L. S., 1977, *J. molec. Struct.*, **38,** 185.
[34] COLOMBO, L., and ZERBI, G., 1980, *J. chem. Phys.*, **73,** 2013.
[35] KINT, S., SCHERER, J. R., and SNYDER, R. G., 1980, *J. chem. Phys.*, **73,** 2599.
[36] ROSENTHAL, L., RABOLT, J. F., and HUMMEL, J., 1982, *J. chem. Phys.*, **76,** 817.
[37] WIBERG, K. B., and MURCKO, M. A., 1988, *J. Am. chem. Soc.*, **110,** 8029.
[38] MAIER, W., and SAUPE, A., 1959, *Z. Naturf.* (*a*), **14,** 882.
[39] HUMPHRIES, R. L., JAMES, P. G., and LUCKHURST, G. R., 1971, *Symp. Faraday Soc.*, **5,** 107.
[40] PALFFY-MUHORAY, P., DE BRUYN, J. R., and DUNMUR, D. A., 1985, *Molec. Crystals liq. Crystals*, **127,** 301.
[41] BATES, G. S., BECKMANN, P. A., BURNELL, E. E., HOATSON, G. L., and PALFFY-MUHORAY, P., 1986, *Molec. Phys.*, **57,** 351.
[42] BATES, G. S., BURNELL, E. E., HOATSON, G. L., PALFFY-MUHORAY, P., and WEAVER, A., 1987, *Chem. Phys. Lett.*, **134,** 161.